

PAPER • OPEN ACCESS

Experimental investigations on the effect of copper on the microstructure and shape memory characteristics of NiTi alloys

Recent citations

- [Wire-EDM machinability investigation on quaternary Ni44Ti50Cu4Zr2 shape memory alloy](#)
C. Balasubramanian *et al*

To cite this article: S Santosh and V Sampath 2020 *IOP Conf. Ser.: Mater. Sci. Eng.* **912** 052009

View the [article online](#) for updates and enhancements.



ECS **240th ECS Meeting**
Oct 10-14, 2021, Orlando, Florida

Register early and save up to 20% on registration costs

Early registration deadline Sep 13

REGISTER NOW

The banner features a photograph of a diverse group of people in a professional setting, smiling and interacting. A diagonal white line separates the text on the left from the image on the right.

Experimental investigations on the effect of copper on the microstructure and shape memory characteristics of NiTi alloys

S Santosh¹ and V Sampath^{1*}

Department of Metallurgical and Materials Engineering, Indian Institute of Technology Madras, Chennai – 600 036, India

E-mail: vsampath@iitm.ac.in

Abstract. Shape memory alloys are fascinating materials, which have exclusively been studied over the last three decades owing to their distinctive functional properties, such as shape memory effect (thermal memory) and superelasticity (mechanical memory). These materials have a unique capability to react to external stimuli, such as heat and stress, because of the reversible martensitic transformation, when subjected to appropriate thermomechanical processing. They find applications in various sectors and are in particular used as actuators and sensors. Among SMAs, NiTi-based alloys are more common and have proven their utility in many practical applications. However, there is still a scope for improvement of the alloys in terms of their shape memory characteristics if they are to be exploited in several other critical applications. In this context, addition of copper proves to be an appropriate element to enhance the transformation characteristics and biocompatibility of NiTi SMAs. Hence, in this work NiTiCu ternary alloys were synthesized by vacuum induction melting followed by subjecting them to suitable thermomechanical treatment. These alloys were then characterized by X-ray diffraction, differential scanning calorimetry and optical microscopy in order to study the influence of copper addition on phases present, transformation temperatures and microstructure of NiTi SMAs. The results are discussed in detail in the paper.

1. Introduction

Shape memory alloys (SMAs) are a distinct group of metallic materials, which undergo solid-to-solid phase transformations, from austenite to martensite and vice versa, in response to stress or temperature [1,2]. These materials show heavy deformation in the martensite phase and regain their initial undeformed shape either on heating (shape memory effect) or on removal of stress at constant temperature (superelasticity) [3, 4]. Shape memory alloys have shown their capabilities in many vital areas and are specially used in most of the major sectors: aerospace, safety, defence, structural, biomedical, robotics, sport, etc. [5-7]. NiTi alloys are the most preferred shape memory materials for many applications since they can accommodate a considerably large distortion in their lattice, which gives rise to shape memory effect. But the lifespan of binary NiTi alloys is limited as they exhibit a broad hysteresis during cycling [8]. The hysteresis can be narrowed down by adding some select alloying elements. Ternary and quaternary addition to Ni-Ti is, by far, the most effective way of altering transformation temperatures [6]. While most of the alloying elements, mostly transition metals, decrease the transformation temperatures, addition of Pd, Pt, Au, Hf, Zr and Cu increase them. In this context, copper proves to be a viable alternative as it easily substitutes for nickel and augments



the workability of the alloy in addition to reducing the hysteresis. Addition of copper also influences the martensitic transformation temperatures and improves corrosion resistance of the alloys [9,10]. When comparing the mechanical properties, ternary NiTiCu alloys have their yield strength almost similar to that of binary NiTi alloys [8].

Various methods have been reported in the literature for the production of thin film and bulk shape memory alloys. Some of them include magnetron sputtering [11, 12], melt spinning [13], vacuum arc remelting [14], vacuum plasma melting [15], flash evaporation [16], molecular beam epitaxy [17], mechanical alloying [18-20], additive manufacturing [8, 21-23] etc. But almost all these methods are suitable for laboratory-scale preparation of bulk alloys and for thin films. For all practical and industrial applications, the alloys have to be prepared in large quantities. Vacuum induction melting (VIM) is an ideal method to produce these special alloys on a large scale. There is still a dearth of literature with respect to vacuum induction melting of NiTiCu alloys. This work therefore discusses the preparation of NiTiCu alloys with varying copper contents via VIM, followed by suitable thermo-mechanical processing and study the influence of copper on the shape memory characteristics.

2. Experimental Procedure

Highly pure raw materials, such as elemental nickel, titanium and copper (each ~ 99.96 wt.% purity) were purchased from M/s. Alfa Aesar in the form of pellets, biscuits and rods. These elements were carefully weighed in suitable quantities according to the composition of the alloy. Five different compositions were used for the study as presented in Table 1. The raw materials were initially cleaned with acetone and then fed into a high density graphite crucible. A special method of arranging the raw materials with titanium cladding at the periphery followed by nickel and copper inside was adapted after Frenzel *et al.* in order to minimize the carbon pick up by the melt [24, 25]. A steel split mould coated with a layer of zirconia for high temperature lubrication was fastened with screws and placed in a resistance furnace for pre-heating at 525 °C for 1h. The preheated mould was then placed carefully in the vacuum chamber of the vacuum induction melting (VIM) furnace to avoid it coming in contact with the induction coil and the chamber was closed. Vacuum was created with the aid of rotary and diffusion pumps in stages to produce a vacuum level of 10^{-5} mbar. After achieving the required level of vacuum the current was switched on in order to heat the charge inside the high density graphite crucible. The temperature rise in the charge was monitored with the help of a Raytek non-contact infrared pyrometer. Once the temperature of the charge reached above 400 °C the chamber was back-filled with argon and a negative pressure was maintained throughout. In order to ensure proper flowability, the heating was continued until the temperature reached ~ 1400 °C and the molten alloy was poured into a preheated steel mould. The mould was then removed from the chamber after giving sufficient time for cooling. The as-cast biscuits were then removed, ground to remove any burrs and sharp corners and then coated with a layer of delta glaze in order to prevent oxidation during subsequent thermo-mechanical treatments. This process was then followed by solutionizing the alloy at 900 °C for 3h. A two-high rolling mill was used in order to reduce 3 mm thick cast biscuits into 1 mm thick sheets. Again the rolled sheet was solutionized at 900°C for 1h and then quenched in water. Samples were then polished to a mirror-finish to remove any adherent delta glaze layer and then cut using an electric discharge machining for further characterization studies. The chemical compositions of the ingots were analyzed using a LECO CS744 Analyzer for carbon and sulphur inclusions, and a LECO ONH 836 Analyzer for oxygen, nitrogen and hydrogen inclusions. The samples were polished using standard metallographic procedures and then etched with an etchant containing nitric acid, hydrochloric acid and hydrofluoric acid for optical microscopy. The phase analysis of the samples was done using a Panalytical X-Ray Diffractometer. The transformation temperatures were evaluated using a Perkin Elmer differential scanning calorimeter with a heating and cooling rate of 10°C/min, respectively and the samples were thermally cycled from – 50°C to 250°C. A Vickers hardness tester (Wolpert Wilson) was employed to determine the hardness of the samples under a load of 0.5 kg for 30 s.

Table 1. Alloy compositions studied in this work.

S.No	Alloy ID	Composition
1	NTCu2	Ni ₄₈ Ti ₅₀ Cu ₂
2	NTCu4	Ni ₄₆ Ti ₅₀ Cu ₄
3	NTCu6	Ni ₄₄ Ti ₅₀ Cu ₆
4	NTCu8	Ni ₄₂ Ti ₅₀ Cu ₈
5	NTCu10	Ni ₄₀ Ti ₅₀ Cu ₁₀

3. Results and Discussion

3.1. CHNOS Analyses

The major impurity elements in binary NiTi shape memory alloys are carbon and oxygen. These impurity elements tend to have a considerable influence on the transformation temperatures and microstructure. They consume titanium in the vicinity by forming titanium carbide and Ti₄Ni₂O_x [25]. Therefore the concentration of average nickel in the matrix increases. As a result, oxygen and carbon take-up should be monitored and kept to a bare minimum, although they cannot be fully suppressed. It is therefore always essential to have a check on carbon and oxygen pick-up by the melt. Hence, the concentrations of carbon, hydrogen, nitrogen, oxygen and sulphur were determined and listed in Table 2.

Table 2. CHNOS results.

Alloy ID	Carbon, wt. %	Hydrogen, wt. %	Nitrogen, wt. %	Oxygen, wt. %	Sulphur, wt. %
NTCu2	0.0276	0.00098	0.000132	0.00155	0.0000535
NTCu4	0.0218	0.00111	0.000327	0.000408	0.0000428
NTCu6	0.0149	nil	0.000114	0.00136	0.0000126
NTCu8	0.0167	0.00127	nil	0.00342	0.0000306
NTCu10	0.0132	0.00119	nil	0.00293	0.0000215

From the results presented in Table 1, it can be seen that carbon and oxygen, which can easily deteriorate the properties of shape memory alloys, are well below 500 ppm, which adheres to the industrial standards. This small amount of carbon can be evidenced because of the special feeding method used as described in the experimental procedure. This helps form a protective TiC layer, which, in turn, reduces the carbon pick-up by the melt. Very low oxygen content in the melt is attributed to the high vacuum levels maintained in the vacuum chamber and also back-filling the chamber with high purity argon gas. All these experimental set-up and precautions are essential in order to produce a sound alloy, which consecutively aids in retaining the shape memory properties of these alloys. The sulphur content is negligible and its presence arises from the initial raw materials used for melting, such as Ni, Ti and Cu.

3.2. X-Ray Diffraction

The X-ray diffractograms of NiTiCu alloys with different compositions at room temperature are shown in Fig. 1. The XRD results were obtained from all alloys after rolling and homogenization at

900°C. The diffractograms obtained at 30°C confirms that there are diffraction lines corresponding to the parent B2 austenite phase. A small peak of martensite is also visible, which is marked as (111). The XRD patterns also reveal the presence of Cu_4Ti_3 precipitate in the matrix. Some other ternary phases of Cu–Ni–Ti intermetallic compounds may also be present, as reported by Pan *et al.* But it must be noted that these compounds are known to possess a similar structure [9]. Therefore separate peaks are not visible.

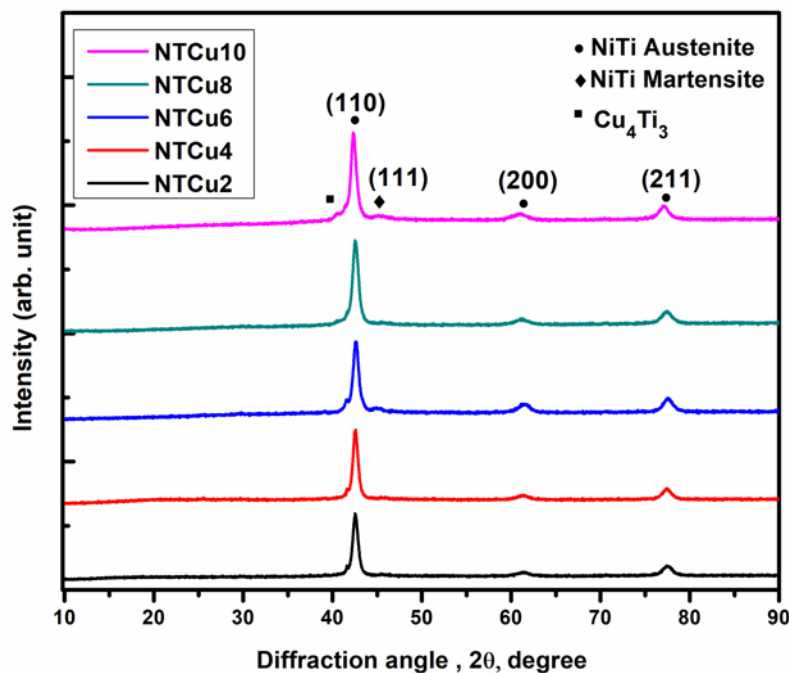


Figure 1. XRD results of NiTiCu alloys.

3.3. Differential Scanning Calorimetry

Figure 2 presents the DSC thermograms of different NiTiCu shape memory alloys. It can be seen that NTCu2, NTCu4 and NTCu10 alloys undergo a single stage $\text{B2} \leftrightarrow \text{B19}'$ transformation during cooling and heating cycles. However, for the other two alloys (NTCu6 and NTCu8) a two-step transformation was evidenced during cooling with the transformation sequence of $\text{B2} \rightarrow \text{R} \rightarrow \text{B19}'$. During the heating cycle, only a single-step transformation ($\text{B19}' \rightarrow \text{B2}$) was observed. R-phase formation is generally not favourable in the case of actuator applications. The R-phase can be avoided completely or partially by varying the composition of the alloy followed by appropriate thermomechanical procedures. The direct martensite formation $\text{B2} \rightarrow \text{B19}'$ with a small hysteresis is essential for actuator applications. With an aim to study the influence of copper on the transformation temperatures, the transformation temperatures were calculated by tangent intersection method and are tabulated in table 3. The transformation temperatures are plotted with increasing copper contents and are presented in Figure 3. There has been almost a steady and consistent increase of all the transformation temperatures with increasing amounts of copper. The addition of copper, therefore, seems to have increased all the transformation temperatures. The increase of copper from 8 to 10 at. % decreases the M_s and M_f temperatures of the alloy though marginally. This decrease can be due to the absence of R-phase transformation and presence of Cu-rich precipitate, which are evident from DSC and XRD, respectively. The variation of hysteresis is shown in Figure 4. It can be observed that the hysteresis width of all alloys is less than 25 °C, which makes these alloys an ideal material for device applications. The hysteresis is very low at 2 at. % and then increases to 21.22 °C mainly because of the appearance of R-phase. Beyond 2 at. %, the hysteresis is maintained constant for the alloys.

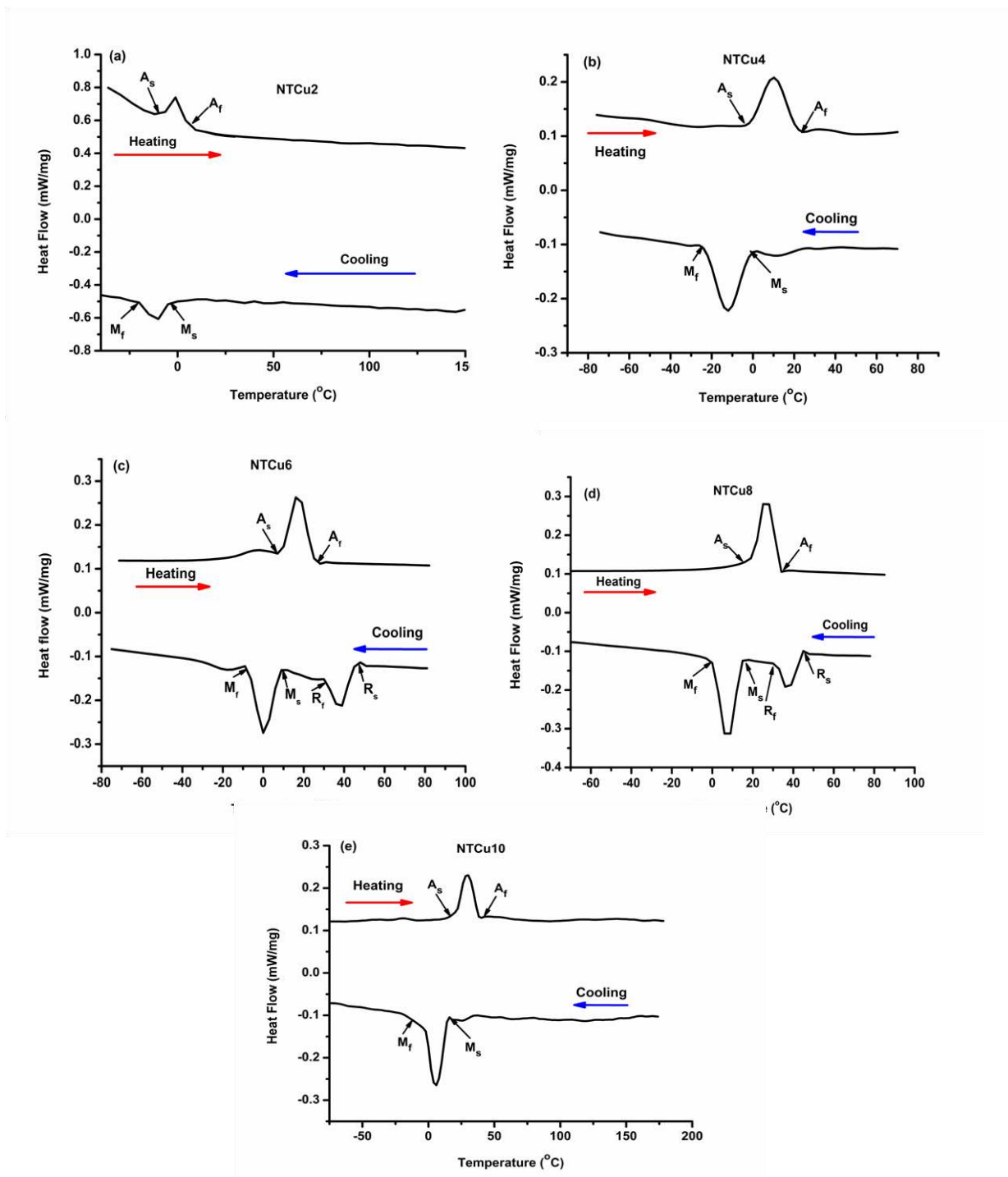
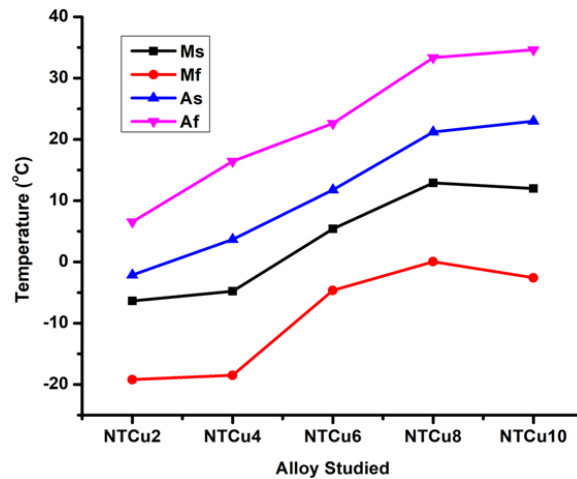
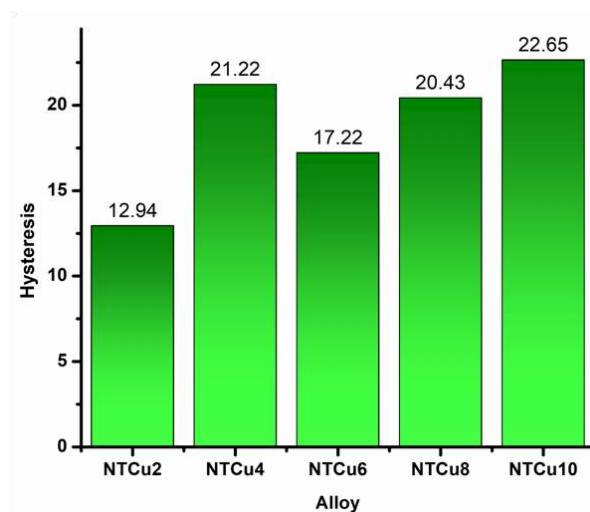


Figure 2. DSC thermograms of (a) NTCu2 (b) NTCu4 (c) NTCu6 (d) NTCu8 and (e) NTCu10 alloys.

Table 3. Transformation temperatures and thermal hysteresis width.

Alloy ID	M_s (°C)	M_f (°C)	A_s (°C)	A_f (°C)	Hysteresis (°C)
NTCu2	-6.38	-19.21	-2.13	6.56	12.94
NTCu4	-4.78	-18.52	3.69	16.44	21.22
NTCu6	5.39	-4.66	11.77	22.61	17.22
NTCu8	12.89	0.022	21.22	33.32	20.43
NTCu10	11.97	-2.6	22.98	34.62	22.65

**Figure 3.** Variation of transformation temperatures with copper content.**Figure 4.** Thermal Hysteresis of the alloys studied.

3.4. Hardness

Figure 5 shows a histogram of Vickers hardness with increasing copper content of the binary NiTi alloys. In shape memory alloys the hardness values are correlated to the transformation temperatures. All the hardness measurements were carried out at room temperature (RT) on the samples that were subjected to an identical heat treatment. Most of the alloys studied have their A_f temperature around RT, i.e. 30 °C. Therefore the hardness values can be taken as a measure of the hardness of these alloys in the austenite phase. Hardness also serves as a promising characterization technique when it comes to shape memory alloys because it directly corresponds to the strength of the sample without causing much damage to the bulk of the sample. From Fig. 7, it is evident that addition of copper enhances the hardness of the alloys because of the formation of copper-rich precipitates, which are evident from XRD. As a result the strength of the austenite phase is also comparatively higher when compared to that in the binary NiTi alloy [26]. Martensite in shape memory alloys is a softer phase. Higher the strength difference between the martensite and austenite phases, higher is the work that is done by the SMA when it recovers. Hence, these NiTiCu SMAs are potential materials for devices with actuators.

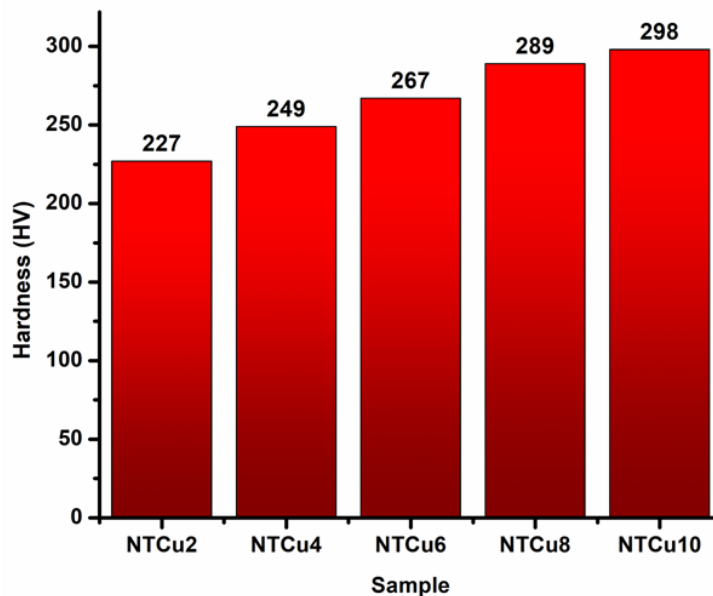


Figure 5. Hardness measurements of different NiTiCu SMAs.

3.5. Microstructure

The micrographs of NiTiCu SMAs with varying copper contents are presented in figure 6. In all cases, martensite plates can be visible throughout the matrix. The martensite plates in the form of needles are finer for lower copper contents and become coarser with higher copper contents. These needle-like martensite plates are oriented along different directions across the matrix. It is also evident from the micrographs that there are many regions of retained austenite which are prominent in all the samples. The distribution of martensite plates in the austenitic matrix is characteristic of NiTi shape memory alloys. The needle-like morphology is favourable for shape recovery [5]. This forms the basis for self-accommodation, which is responsible for shape recovery in these alloys.

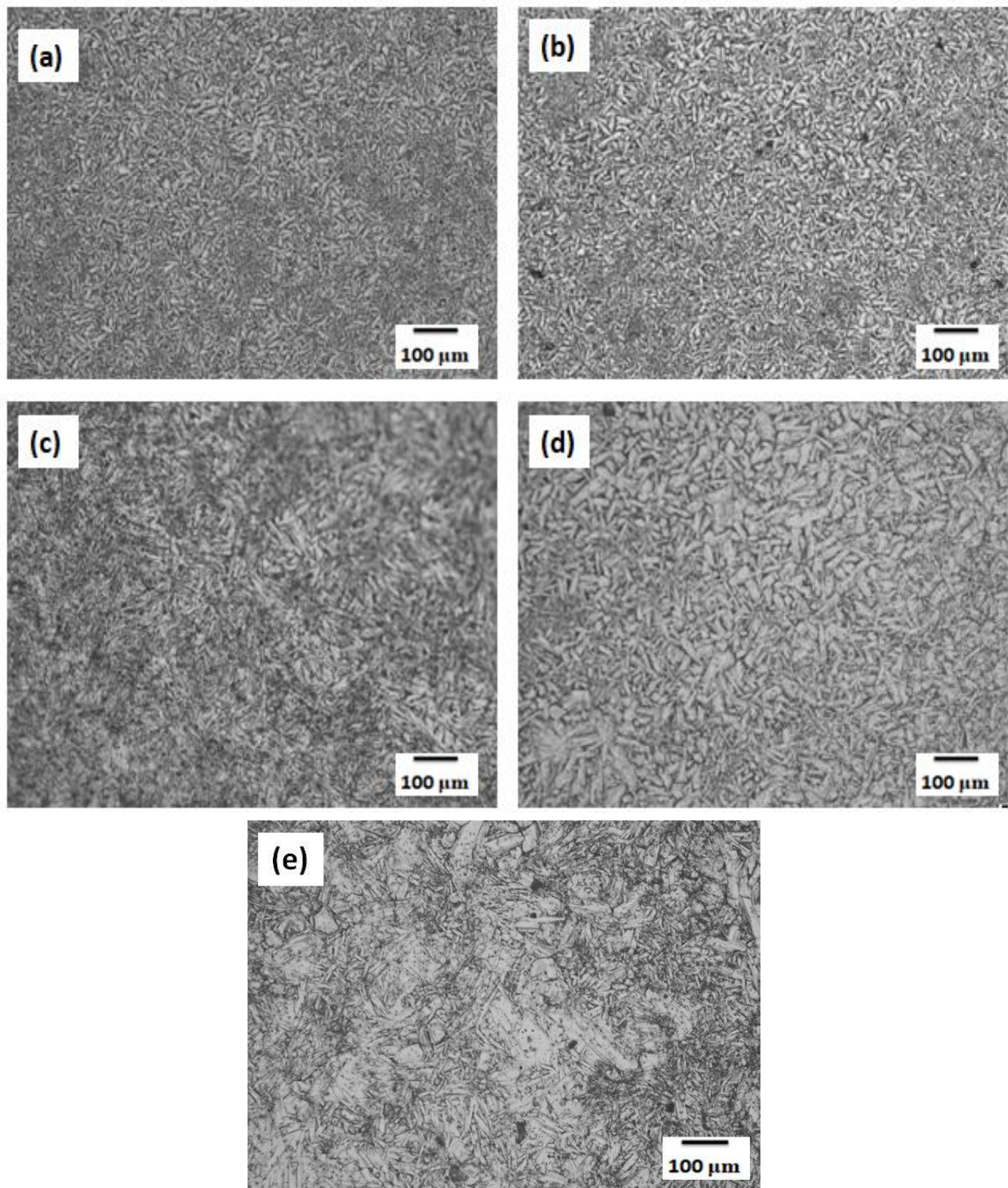


Figure 6. Micrographs of (a) NTCu2, (b) NTCu4, (c) NTCu6, (d) NTCu8 and (e) NTCu10 alloys.

4. Conclusions

NiTiCu (Cu - 2, 4, 6, 8, 10 at. %) SMAs were successfully fabricated by vacuum induction melting. They were then subjected to appropriate thermo-mechanical processing to obtain the best properties and the samples were characterized using different techniques. Following conclusions can be drawn from this study:

CHNOS analysis confirms that carbon and oxygen impurities, which have proven to deteriorate the properties of SMAs, are present within permissible limits in all these alloys.

X-Ray diffractograms signify that alloying has taken place properly and the austenite peaks were prominent along with faint martensite peaks.

Differential scanning calorimetry reveals that copper addition increases almost all the transformation temperatures. Presence of two-step transformation (B2 → R → B19') in some alloys is also evident.

Hardness steadily increases with copper addition. This can be attributed to the formation of Cu-rich precipitates.

The microstructure confirms the presence of needle-like martensite distributed in an austenitic matrix.

All the above results indicate that NiTiCu alloy can be an actuator material for any kind of application.

The transformation temperatures and R-phase formation can be tailored by choosing appropriate alloy contents and thermo-mechanical processing.

5. References

- [1] Arunkumar S, Kumaravel P, Velmurugan C and Senthilkumar V 2019 *Materials Research Express* **6** 105708
- [2] Jani J M, Leary M, Subic A and Gibson M A 2014 *Materials and Design* **56** 1078-113
- [3] Sanusi K O, Ayodele O L and Khan M T 2014 *South African Journal of Science* 110 1
- [4] Otsuka K and Ren X 1999 *Intermetallics* **7** 511
- [5] Wayman C M 1993 *MRS Bulletin* **18** 49
- [6] Santosh S and Sampath V 2019 *Transactions of the Indian Institute of Metals* **72** 1481
- [7] Humbeeck J V 1999 *Materials Science Engineering* **134** 273–275
- [8] Shiva S, Palani I A, Paul C P, Mishra S K and Singh B 2016 *Journal of Materials Processing Technology* **238** 142.
- [9] Pan G, Balagna C, Martino L, Pan J and Spriano S 2014 *Journal of Alloys and Compounds* 589 633.
- [10] Li H F, Qiu K J, Zhou F Y, Li L and Zheng Y F 2016 *Scientific Reports* **6** 37475
- [11] Ren M H, Wang L, Xu D and Cai B C 2000 *Materials and Design* **21** 583
- [12] Cai M, Fu Y Q, Sanjabi S, Barber Z H and Dickinson J T 2007 *Surface and Coatings Technology* **201** 5843
- [13] Mehrabi K, Bruncko M and Kneissl A C 2012 *Journal of Alloys and Compounds* 526 45
- [14] Nespoli A, Passaretti F and Villa E 2013 *Intermetallics* **32** 394
- [15] de Araújo C J, da Silva N J, da Silva M M and Gonzalez C H 2011 *Materials and Design* **32** 4925
- [16] Mineta T, Deguchi T, Makino E, Kawashima T and Shibata T 2011 *Sensors and Actuators A* **165** 392
- [17] Ralf H, Jurgen F, Rene P, Sigurd T, Markus B, Tobias S, Bernhard V and Michael M 2006 *Materials Transactions* **43** 933
- [18] Fatemeh A, Rasool A, Mohammad G, Morteza A and Ali K O, 2014 *Materials and Design* **55** 373
- [19] Ghadimi M, Shokuhfar A, Zolriasatein A and Rostami H R 2013 *Materials Letters* 90 30
- [20] Velmurugan C and Senthilkumar V 2018 *Journal of Alloys and Compounds* 767 944
- [21] Moghaddam N S, Saedi S, Amerinatanzi A, Hinojos A, Ramazani A, Kundin J, Mills M J, Karaca H and Elahinia M 2019 *Scientific Reports* **9** 41
- [22] Humbeeck J V 2018 *Shape Memory and Superelasticity* **4** 309

- [23] Haberland C, Elahinia M, Walker J M, Meier H and Frenzel J 2014 *Smart Materials and Structures* **23** 104002
- [24] Frenzel J, Zhang Z, Neuking K and Eggeler G 2004 *Journal of Alloys and Compounds* **385** 214
- [25] Zhang Z, Frenzel J, Neuking K and Eggeler G 2006 *Materials Transactions* **47** 661
- [26] Fuentes J M G, Gümpel P and Strittmater J 2002 *Advanced Engineering Materials* **4** 437